International Journal of Pharmaceutics 694 (2026) 126735

Contents lists available at ScienceDirect

International Journal of Pharmaceutics

journal homepage: www.elsevier.com/locate/ijpharm

# Injectable biodegradable silica hydrogel depot for dexamethasone delivery in the eye via subconjunctival administration

Ville-Matias Pollari [a,b,*], Annika Valtari [b], Lauri Marttila [a], Kati-Sisko Vellonen [b], Marceline Akieh-Pirkanniemi [a], Mika Jokinen [a,**], Lasse Leino [a,c], Astrid Subrizi [b], Arto Urtti [b]

[a] DelSiTech Ltd., Itäinen Pitkäkatu 2 C, 20520 Turku, Finland
[b] School of Pharmacy, Faculty of Health Sciences, University of Eastern Finland, Yliopistonranta 8, FI-70210 Kuopio, Finland
[c] Department of Life Technologies, University of Turku, Turku, Finland

ARTICLE INFO

*Keywords:*
Subconjunctival injection
Biodegradable silica
Ocular drug delivery
Dexamethasone
Pharmacokinetic simulation

ABSTRACT

This preclinical study evaluated feasibility of an injectable biodegradable silica hydrogel depot formulation for subconjunctival drug delivery into the eye utilizing dexamethasone as active component. The silica hydrogel formulation was manufactured using spray-dried silica microparticles with encapsulated dexamethasone which were mixed with a silica hydrogel to form a continuous solid phase within an aqueous liquid phase. The formulation was then analyzed for dexamethasone and silica contents, rheology, injectability, as well as *in vitro* dissolution of dexamethasone and silica. Finally, the formulation was studied for pharmacokinetics and release of dexamethasone in the rabbit after subconjunctival injections for 26 days. Dexamethasone and silica release profiles *in vitro* and *in vivo* were compared with pharmacokinetic simulations made *in silico*. Dexamethasone was efficiently encapsulated within a visually white, homogenous, shear thinning and injectable hydrogel consisting of silica microparticles with an average diameter of 2.5 μm and a span of 3.5 μm. The hydrogel depot dissolved completely *in vitro* in sink in few days. In the rabbit study dexamethasone levels were measurable in both plasma and vitreous up to 26 days post injection. Pharmacokinetics was modelled in silico and a predictive tool was generated to support iterative formulation development. Silica hydrogel depot is a promising carrier material for subconjunctival injection of dexamethasone. Pharmacokinetic modelling is a useful tool for optimization of subconjunctival controlled release formulations and for refining the design of animal studies.

**Chemical compounds studied:** Dexamethasone, Silicic Acid, Non-porous Silica.

## 1. Introduction

Topical eye drop administration of dexamethasone is routinely used to treat inflammatory eye diseases in the anterior segment. However, due to the ocular tissue barriers and the rapid elimination of eye drops from the ocular surface, the ocular bioavailability of dexamethasone is low (≈0.1 %) (Gaudana et al., 2010; Järvinen et al., 1995; Naageshwaran et al., 2022; Ranta and Urtti, 2006) and its duration of action is short. Consequently, frequent instillation is required (1–2 drops every 4–6 h up to hourly dosing), which increases the risk of adverse effects, such as cataract formation and elevated ocular pressure (Grzybowski et al., 2019; Thorne et al., 2010). Prolonged duration of action is needed to improve the therapeutic efficacy of ocular dexamethasone treatments. In general, achieving long-lasting action with eyedrops is challenging, even with improved formulations, whereas subconjunctival injection may enable longer retention and remarkably extended duration of action. (Rafiei et al., 2020).

Corticosteroid treatment of the posterior eye segment is accomplished currently with intravitreal injections of suspensions or implants. Commercial biodegradable dexamethasone implant (Ozurdex®) produces vitreous and retinal drug levels ranging from 0.1 μg/ml to several μg/ml for about one month (Bhagat et al., 2014; Won et al., 2024). Likewise, injectable sustained-release particulate systems (e.g., PLGA nanoparticle formulations in rabbits) can produce vitreous concentrations in the μg/mL range around 3–4 weeks (Zhang et al., 2009). These levels are much higher than the suggested minimal therapeutic threshold concentration (≈ 1 nM) (Annala et al., 2025; Chang-Lin et al., 2011; Nauck et al., 1998; Sadeghi et al., 2022). Thus, intravitreal formulations may result in much higher drug levels than needed. High

* Corresponding authors.
*E-mail addresses:* villpoll@uef.fi (V.-M. Pollari), mika.jokinen@delsitech.com (M. Jokinen).

https://doi.org/10.1016/j.ijpharm.2026.126735
Received 22 December 2025; Received in revised form 27 February 2026; Accepted 28 February 2026
Available online 2 March 2026

**Glossary**

| Term | Definition |
|---|---|
| API | Active pharmaceutical ingredient |
| AUC | Area Under the Curve |
| CL | Clearance |
| HPLC | High-Performance Liquid Chromatography |
| IVT | Intravitreal |
| $k_{a,1,2,etc.}$ | Release rate constant |
| LC-MS | Liquid Chromatography–Mass Spectrometry |
| MP-AES | Microwave Plasma – Atomic Emission Spectroscopy |
| SEM | Scanning electron microscope |
| TEOS | Tetraethyl-orthosilicate |

intravitreal concentrations of dexamethasone involve risks, such as increased intraocular pressure and development of cataract (Chan et al., 2011; Goñi et al., 2016; Kiddee et al., 2013).

Established controlled release platforms for parenteral dosing include non-biodegradable polymers (e.g., ethylene vinyl acetate, polyvinyl alcohol) and biodegradable polymers (e.g., poly lactic-co-glycolic acid, polycaprolactone) (Thrimawithana et al., 2011; Walvekar et al., 2023; Wang et al., 2023, 2025). However, many systems have limitations, such as low drug loading capacity, initial burst release and acidic degradation byproducts (McGowan et al., 2024; Tyagi et al., 2018; Wang et al., 2023). Furthermore, some systems may induce local irritation or degradation-related complications (Go et al., 2020).

Biodegradable silica-based formulations have attracted growing interest as robust and versatile platforms for sustained drug delivery (McGowan et al., 2024; Tyagi et al., 2018). These systems have demonstrated excellent compatibility as well as sustained and tunable release (Al-Kinani et al., 2018; Kortesuo et al., 2000), making them promising candidates for ocular drug delivery. Usually, these so-called depot systems consist of spray-dried silica microparticles embedded in colloidal silica hydrogel (Forsback et al., 2021; Jokinen et al., 2018; McGowan et al., 2024; Noppari et al., 2021; Tyagi et al., 2022; Viitala et al., 2005b, 2005a). The hydrogel exhibits shear-thinning properties upon injection and provides erosion-controlled drug release (Forsback et al., 2021; Jokinen et al., 2018; McGowan et al., 2024; Viitala et al., 2005b). Therefore, it differs from non-modified mesoporous silica that releases drug mainly by diffusion (Benkő et al., 2025). The rates of non-porous silica matrix degradation and drug release can be tuned by modulating the density of surface hydroxyl groups and the degree of silica condensation (Forsback et al., 2021). Lack of pH changes at the site of injection is a notable advantage over PLGA-based systems (Lu et al., 2023; Wang et al., 2025). Controlled release of small molecules, peptides, proteins, and oligonucleotides from silica-based systems for weeks or months have been reported *in vitro* and *in vivo* after subcutaneous administration (McGowan et al., 2024; Tyagi et al., 2018).

Subconjunctival injection is a viable approach for drug delivery to the anterior segment of the eye, and possibly also for the posterior segment. Compared with intravitreal injections, subconjunctival injections are less invasive and associated with a lower risk of complications (Rafiei et al., 2020; Thrimawithana et al., 2011). Subconjunctivally administered systems may therefore improve patient compliance and treatment outcomes (Al-Kinani et al., 2018; Silva et al., 2021).

In this study, an injectable, sustained release dexamethasone silica depot formulation was developed and characterized in terms of physical parameters and *in vitro* drug release properties. Moreover, the formulation was administered in the subconjunctiva of the rabbit eye to investigate preliminary pharmacokinetics. The study – demonstrates for the first time – the feasibility of an injectable, biodegradable silica hydrogel depot for local, subconjunctival dosing.

## 2. Materials and methods

### 2.1. Materials

Dexamethasone from AK Scientific (batch LC401228U1) was used as the active pharmaceutical ingredient in injectable formulations. Tetraethyl orthosilicate (reagent grade), precursor for the silica sol was purchased from Merck (St. Louis, MO, USA) and prefiltered prior to use with Teflon (PTFE-S) 0.2 μm filter. Hydrochloric acid and sodium hydroxide solutions were bought from Merck (Germany) and were filtered prior to use with cellulose acetate (CA-S) 0.2 μm filter. Ethanol was supplied by Anora (Finland). Silica standard solution (1000 μg/mL) was from Thermo Fisher (Germany). Trifluoroacetic acid from VWR (United Kingdom), methanol was supplied by Honeywell (Germany) and Tris (hydroxymethyl)aminomethane was supplied by VWR (Belgium). Ammonium bifluoride was supplied by Acros Organics (Germany).

### 2.2. Preparation of silica hydrogel depot formulations

The silica hydrogel depots were manufactured according to methods described earlier (Forsback et al., 2021). First, the silica sol for silica microparticles was prepared by an acid catalytic hydrolysis reaction of tetraethyl orthosilicate (TEOS) in deionised water at pH 2.0 (pH was adjusted with 0.1 M HCl). Molar ratio of TEOS:water was 1:10. Hydrolysis reaction was carried out at room temperature for 25 min. The resulting silica sol was cooled to +5 °C in an ice bath before mixing with the dexamethasone solution. Dexamethasone was dissolved in ethanol (total volume was 109 mL) to yield a concentration of 1.85 mg/mL. The dexamethasone solution was combined with 27.1 mL of the silica sol. The pH of the dexamethasone-silica sol mixture was adjusted to 6.1 with 0.1 M sodium hydroxide before pumping it to a spray-dryer.

A Buchi B-290 (Büchi AG, Flawil, Switzerland) spray dryer with manual nozzle gap of 1.4 mm was used. The spray drying parameters were as follows: aspirator air flow rate was 100 % (approximately 35 $m^3$/h) with maximum atomization air, fluid flow rate 20 % (ca. 5.6 mL/min) and constant inlet temperatures of 100 °C. The outlet temperature was typically in the range of 50–53 °C. These values were recorded every five minutes during the 20 min of spray drying.

To produce the injectable biodegradable dexamethasone-silica hydrogel depot formulation, (later referred as 'formulation' or 'silica-hydrogel depot') spray dried dexamethasone-silica microparticles were suspended in a dilute silica sol. Target dexamethasone load in injectable silica-hydrogel depot was 0.48 mg/mL. The concentration of dexamethasone-silica microparticles in the suspension as mass percentage was 43 wt%. Other part of the suspension contains several components, i.e. silica, water and ethanol. The dilute silica sol was prepared with an acid catalysis reaction as described above but the molar ratio of TEOS:water was 1:400. The pH of the dilute silica sol was adjusted to 6.1 prior to the suspension preparation. The suspension was transferred into 0.5 mL Gerresheimer glass syringes (Wirth Emballage, Sweden) and placed in constant custom-made tube rotator for four days to ensure homogenous gel formation. The pH of the formulation was confirmed by measuring it in a water mixture.

### 2.3. Particle size measurements and scanning electron microscopy

Laser diffraction technique (Static Light Scattering, SLS) was used in microparticle size distribution analysis. The equipment used was a Sympatec HELOS BR3 using R3 lens and the measurement range was from 0.5 to 175 μm. Ethanol was used as a dispersant.

The scanning electron microscopy (SEM) images were taken from microparticles with JCM-7000 SEM.

### 2.4. Rheological measurement and manual injectability test

The injectability of the silica-hydrogel depot was assessed by

manually ejecting the substance from 0.5 mL Gerresheimer syringes through a 23 G needle. The dynamic viscosity and viscoelastic properties of the formulations were analyzed using the Anton Paar MCR 302 rheometer (Austria), as described previously (McGowan et al., 2024; Noppari et al., 2021). All measurements were obtained with three parallel samples from the same syringe.

### 2.5. Silica and dexamethasone assay

Dexamethasone was extracted from the formulation by dissolving the matrix in 1 M ammonium bifluoride solution at room temperature. A sample was analyzed for dexamethasone with high performance liquid chromatography (HPLC) using 1260 Infinity HPLC from Agilent with XBridge Premier BEH C18, 2.1 x 100 mm, 2.5 μm (Waters) column. The separation in the column was achieved by a gradient run for 2 min from 40 to 80 % of Eluent B. Eluent A was 0.1 % trifluoroacetic acid and Eluent B was methanol. A diode array detector (DAD) set at 242 nm was used for detecting dexamethasone in the sample solution.

Microwave plasma atomic emission spectroscopy from Agilent (MP-AES, model 4210 coupled with OneNeb nebulizer) was used to detect and quantify the dissolved silica (silicic acid) in the sample solutions (materials and methods 4.6, 4.8.2 and 4.8.3). The detection wavelength of 251.6 nm for silicon was used. Linear quantitation range of the method was from 0.1 to 25 μg/mL and the detection limit was 0.05 μg/mL. All the silica measurements were done against silica standards and thus results are presented as silica instead of silicic acid.

### 2.6. In vitro dissolution test

The *in vitro* release kinetics of dexamethasone and dissolution rate of silica from the dexamethasone-silica microparticles and from the silica-hydrogel depot were determined using an accelerated *in vitro* dissolution testing method. The *in vitro* dissolution method was designed to maintain *sink* conditions for silica, as described earlier (Tyagi et al., 2018). The *sink* condition was maintained by replacing the dissolution medium with fresh dissolution buffer at each sampling time. Three parallel tests were conducted with 10–15 mg of dexamethasone-silica microparticles (20–30 mg of silica-hydrogel formulation) in 50 mL 50 mM Tris-buffer (pH 7.4 at 37 °C) as the dissolution medium. The study was performed in 60 mL polypropylene (PP) vessels in a shaking water bath at 37 °C and 60 S/minute (spm). At predetermined times (1, 3, 5, 7, 12, 24, 48, 72 and 120 h), the samples were withdrawn and centrifuged at 3808 g for 5 min. Then, 20 mL of the supernatant was collected for analysis. The remaining supernatant was discarded, and the sediment was resuspended in fresh dissolution medium (50 mL) and transferred to the water bath at 37 °C and 60 spm until the next timepoint. The samples were analyzed for dexamethasone and silica as described (section 3.5). Cumulative amounts of dissolved dexamethasone and silica were calculated.

### 2.7. Encapsulation efficiency test

Spray dried silica microparticles containing dexamethasone were suspended in ethanol at 1:1 (m:w) ratio (approximately 10 mg of microparticles and 10 mL of ethanol) and shaken at room temperature overnight at 65 spm. Suspension was then centrifuged at 3808 g for 5 min. Supernatant (0.2 mL) was collected and diluted 1:5 (0.2 mL + 0.8 mL) into 50 mM Tris buffer before quantification of dexamethasone (see section 2.5.).

### 2.8. In vivo pharmacokinetic study in the rabbit

#### 2.8.1. Animals

*In vivo* study with the silica-hydrogel depot was performed with three adult New Zealand White female rabbits (weighing 3.6–4.1 kg) from Envigo Laboratories (UK) in Ocular Drug Development Laboratory in Laboratory Animal Center, University of Eastern Finland (Kuopio, Finland) (license (ESAVI/27769/2020; EU directive 2010/63/EU). The animals were housed under standard laboratory conditions of 12 h dark-light cycles and were provided with normal pellet and hay diet with water *ad libitum*. The animals were handled in accordance with the statement of the Animals in Research Committee of the ARVO (Association for Research in Vision and Ophthalmology, Rockville, Maryland, USA).

#### 2.8.2. Dosing and sampling

The silica-hydrogel depot (59 μL/eye) was injected under the bulbar conjunctiva at the supero-temporal site of each rabbit eye. The appropriate injection site was confirmed by stereo microscope (Leica® S9D, MC170 HD, Leica Microsystems IR GmbH) that was also used for visual monitoring of the depot throughout the study.

Before the injections the rabbits were anaesthetised with medetomidine (Domitor vet® 1 mg/mL, Orion Corp.) and ketamine (Ketaminol vet® 50 mg/mL, Intervet International B.V.) with dosage of 0.4 mL/kg, subcutaneous (sc), and the ocular surface was treated with local anaesthetic oxybuprocaine (Oftan Obucain® 4 mg/mL, Santen Pharmaceutical Co., Ltd.). During the anaesthesia the ocular surface was moisturised with carbomer (Viscotears® 2 mg/g, Dr. Gerhard Mann Chem.-Pharm. Fabrik GmbH).

Subconjunctival injections were performed with 23G regular wall needle (Henke-Ject®, 23Gx1″, 0.6x25mm, lot# 14–15201). Prior to administration into the subconjunctival space (supero-temporal quadrant of bulbar conjunctiva), the formulation in the Gerresheimer glass syringe was meticulously primed to achieve a volume of 59 ± 3 μL. This priming process was executed with a custom-made dose assisting device to ensure accurate dosing. An example photo of the silica-hydrogel depot in the subconjunctival space post dosing is attached as supplemental material (Fig. S1).

After the ocular injections the animals received prophylactic pain relief (Rimadyl Bovis vet®, carprofen 50 mg/mL, Zoetis Animal Health ApS) of dosage 0.08 mL/kg, sc, and the anaesthesia was antagonized with atipamezole (Antisedan vet®, atipamezole 5 mg/mL, Orion Corp.) of dosage 0.2 mL/kg, sc.).

Tear fluid and plasma samples were collected at predefined times (1, 3, 7, 11, 14, 20 and 26 days post-dosing) from the rabbits placed in restrainers. Ten minutes prior to blood sampling the rabbit ears were treated with local anesthesia (EMLA® cream, lidocaine and prilocaine 25/25 mg/g, Aspen Nordic) to prevent pain. The blood samples were collected from the ear arteria to blood collection tubes (BD vacutainer® K2E Plus, Bellevier Industrial Estate, Plymouth, UK) with a 25G needle. Approximately 30 min before tear fluid sampling carbomer gel was gently rinsed from the ocular surface with 0.9 % sodium chloride. Tear fluid samples (3 μL/sample) were collected with glass capillaries from the lower fornix. After the tear fluid sampling at 3.5 h and 24 h timepoints prophylactic topical antibiotic (Oftan Chlora®, chloramphenicol 10 mg/g, Santen Pharmaceutical Co., Ltd.) was applied on the ocular surface.

At the end of the experiment, each rabbit was anesthetised as described previously and euthanized with intravenous pentobarbital (Euthoxin vet® 500 mg/mL, Chanelle Pharmaceuticals Manufacturing Ltd, Galway, Ireland; 1 mL/1.5 kg). Vitreous humour and aqueous humour were collected with needle suction and the silica-hydrogel depot remnant was collected with scalpel and forceps for further analysis.

#### 2.8.3. Analytics

Dissolved silica in the rabbit tear fluid samples was measured spectrophotometrically (820 nm) using molybdenum blue complex method (Coradin et al., 2004). The method was adapted to 96 well plate format so that the final volume per well was 100 μl (adjusted with milliQ-water) and reagents used were scaled according to that. Limit of detection was 0.055 μg/mL and limit of quantitation was 0.55 μg/mL for the concentration in the well.

Dexamethasone concentrations in the rabbit tear fluid, plasma, aqueous humour and vitreous humour samples were determined using LC-MS/MS (Agilent 1290 series liquid chromatograph coupled with an Agilent 6495 triple-quadruple mass spectrometer equipped with an electrospray ionization source) according to the previously published methods (Balla et al., 2022; Valtari et al., 2024). Briefly, the tear fluid samples were first diluted 1:20 with the internal standard solution (40 ng/mL dexamethasone-d5 in 1 % formic acid and 50 % acetonitrile) and then centrifuged at 14,000 rpm for 10 min at + 4 °C. Supernatants were collected for LC-MS/MS analyses. The plasma samples were prepared according to the methyl t-butyl ether extraction procedure described previously. (Valtari et al., 2024).

For the chromatographic separation of dexamethasone an InfinityLab Poroshell 120 SB-C18 (2.1 x 50 mm, 2.7 μm) column (Agilent) was used. The mobile phase consisted of 0.1 % formic acid (Eluent A) and methanol (Eluent B). The flow rate was 0.5 mL/min with the following gradient 0.0–2.5 min: 30 %→100 % B, 2.5–3.0 min: 100 % B, 3.0–3.1 min: 100 %→30 % B, 3.1–4.5 min 30 % B. The injection volume was 2 μL or 10 μL and column was maintained at a temperature of 50 °C.

Mass spectrometry detection was performed in positive ion mode using following multiple reaction monitoring (MRM) transitions and collision energies (CE): 393.0 −> 373.0 (CE 4) and 393.0 −> 355.1 (CE 12) for dexamethasone, and 398.0 −> 378.1 (CE 8) and 398.0 −> 360.2 (CE 8) for internal standard dexamethasone-d5. Limit of quantitation (LOQ) was 0.1 ng/mL for plasma and tear fluid, and 0.02 ng/ml for vitreous- and aqueous humours.

The silica-hydrogel depot remnants were collected from subconjunctival space of the rabbits 26 days after injection. The remnant was cut to smaller pieces with scalpel. The pieces were washed with 4 mL of Tris-buffer to a polypropylene vessel and 2 mL of 1 M ammonium bifluoride ($NH_4HF_2$) and 1 mL of ethanol were added, and the vessel was shaken for 20 min at room temperature in tabletop shaker. Then, the sample was centrifuged at 3803 g for 5 min and 4 mL of the supernatant was collected fully. 1 mL of supernatant was provided for silica measurement by Microwave Plasma – Atomic Emission Spectroscopy (MP-AES). Another 1 mL of supernatant was collected for HPLC analysis and for this 100 μl of 10 % syloid (Grace Gmbh & Co. KG, Germany) was used to neutralize remaining $NH_4HF_2$ in the supernatant. Neutralized sample was centrifuged at 12,400 g for 5 min and 1 mL of supernatant was transferred to HPLC vials for dexamethasone analysis as described in section 3.5. To confirm the total extraction of silica the remaining pellet was resuspended with the addition of 2 mL of Tris-buffer, 3 mL of 1 M ammonium bifluoride solution and 1 mL of ethanol. The solution was shaken (at room temperature) overnight to ensure complete dissolution of the material. After complete dissolution the sample was diluted with addition of 4 mL of Tris-buffer and then centrifuged as before and supernatant collected for analysis as described in section 3.5.

### 2.9. Pharmacokinetic simulations

Simulations were performed with STELLA software (version 10.0.4 utilizing Runge-Kutta 4 integration with DT of 0.02) to model *in vitro* and *in vivo* drug release, dissolution of silica, and systemic absorption of dexamethasone. Schematic structure of the model is shown in Fig. 1 and the parameters are in Table 1. The two-compartmental pharmacokinetic model of dexamethasone in plasma is based on the prior study (Valtari et al., 2024).

## 3. Results and discussion

### 3.1. Silica-dexamethasone microparticle characteristics

The silica-hydrogel depot consisted of spray-dried silica microparticles with encapsulated dexamethasone embedded in a colloidal silica-hydrogel. The silica and dexamethasone contents in the microparticles were 73.2 % (w/w) and 4.4 % (w/w), respectively. The rest of the

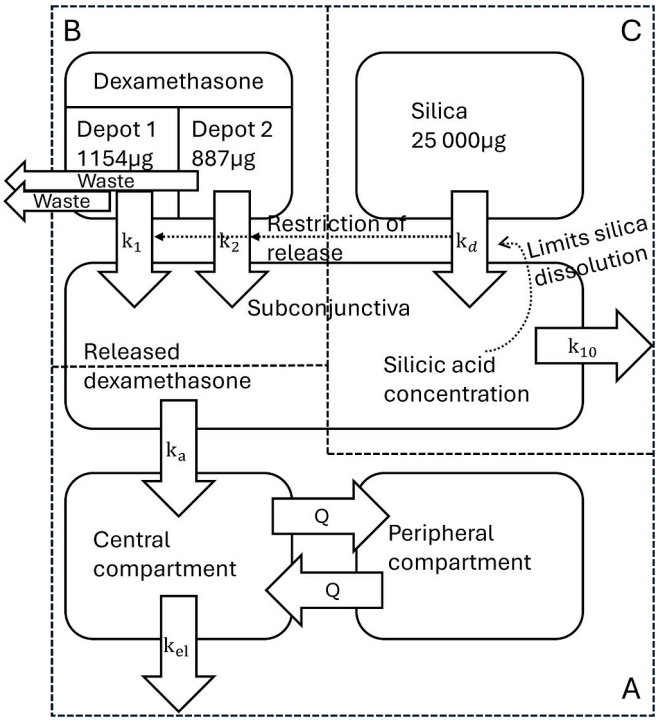


**Fig. 1.** Simulation model for silica-hydrogel formulation administered into subconjunctival space in rabbits. Section A is PK-model based on Valtari et al. 2024., section B incorporates drug release kinetics based on experimental data and section C introduces silica dissolution into the model.

microparticle mass consists mostly of water entrapped in the matrix. Visually the microparticles were white or almost white powder.

The encapsulation efficiency of dexamethasone in silica microparticles was 98.3 % (i.e. 1.7 % of the drug being outside the matrix). Encapsulation efficiency depends on the properties of the drug and other manufacturing parameters of the sol processing step. Previously, encapsulation efficiency of 83.0–99.2 % was reported for bevacizumab in silica microparticles after spray-drying manufacture (Noppari et al., 2021). High encapsulation efficiency is important for applications requiring low burst release.

The particle size distribution of the dexamethasone-silica microparticles showed a single and relatively narrow peak. The span (D90-D10)/D50 was 3.54 ± 0.10, with only minor shoulder peaks (<5 %) between 20–50 μm (Fig. 2). Particle sizes are presented as D-values (D10, D50, D90), indicating that 10 %, 50 % and 90 % of particles are smaller than the corresponding sizes, respectively. The D90 was 9.59 ± 0.26 μm (mean ± SD), D50 2.48 ± 0.00 μm and D10 was 0.80 ± 0.00 μm.

The particle size distribution of the microparticles is also important for the injectability of silica-hydrogel depot, as larger particles may require higher injection forces and may lead to needle blockade (Rungseevijitprapa and Bodmeier, 2009; Zhao et al., 2023). Silica-hydrogel formulations with similar particle size distributions have been shown to provide good injectability through 25G needles (Tyagi et al., 2018). Scanning electron microscopy (SEM) images showed round particles (Figs. S2 and S3, supplemental material).

### 3.2. Drug loading and rheological properties of silica-hydrogel depot

Total dexamethasone content in the silica-hydrogel depot was 1.8 % (w/w). The measured concentrations of dexamethasone and silica in the hydrogel depot were 20.85 ± 0.02 mg/mL and 384.75 ± 2.69 mg/mL, respectively. Visually, the silica-hydrogel depot was white or almost white, homogeneous and semisolid material, where no phase separation or microparticle sedimentation was observed.

**Table 1**
Parameters for subconjunctival delivery of dexamethasone in silica-hydrogel formulation in rabbits.

| Parameter abbreviation | Description | Unit | Source/value |
|---|---|---|---|
| $A_1$ | Dexamethasone amount in the central body compartment | µg | Model variable |
| $A_2$ | Dexamethasone amount in peripheral body compartment | µg | Model variable |
| $A_{sc}$ | Released dexamethasone in the subconjunctival space | µg | Model variable |
| $J_{01}$ | Rate of drug absorption from subconjunctival space to plasma | µg/h | $F*A_{sc}*k_a$ |
| $J_{12}$ | Distribution rate of drug from central to peripheral compartment | µg/h | C*Q |
| $J_{21}$ | Distribution rate of drug from peripheral to central compartment | µg/h | $C_p*Q$ |
| $J_{10}$ | Elimination rate of drug | µg/h | CL*C |
| C | Concentration of dexamethasone in plasma | µg/ml | $A_1/V_1$ |
| CL | Plasma clearance of dexamethasone | ml/h | 943 (Valtari et al., 2024; weight adjusted) |
| $C_p$ | Concentration of dexamethasone in peripheral compartment | µg/ml | $A_2/V_2$ |
| F | Fraction of soluble dexamethasone absorbed from subconjunctival space to plasma | – | 0.993 (Valtari et al., 2024) |
| $k_a$ | Absorption rate constant of soluble dexamethasone | 1/h | 2.58 (Valtari et al., 2024) |
| Q | Distribution clearance between plasma and peripheral compartments | ml/h | 1350 (Valtari et al., 2024; weight adjusted) |
| $V_1$ | Volume of central compartment | ml | 1926 (Valtari et al., 2024; weight adjusted) |
| $V_2$ | Volume of peripheral compartment | ml | 724 (Valtari et al., 2024; weight adjusted) |
| Weight | Rabbit body weight (mean) | kg | 3.89 |
| **$D_1$** | Fast releasing fraction of dexamethasone in depot | µg | 1154 |
| $D_2$ | Slow releasing fraction of dexamethasone in depot | µg | 887 |
| $J_F$ | Fast dexamethasone release rate (from $D_1$) | µg/h | $R*D_1*(1-F_{loss})*k_1$ |
| $J_{F,\ loss}$ | Fast dexamethasone loss rate (from $D_1$) | µg/h | $R*D_1*F_{loss}*k_1$ |
| $J_S$ | Slow dexamethasone release rate (from $D_2$) | µg/h | $R*D_2*(1-F_{loss})*k_2$ |
| $J_{S,\ loss}$ | Slow dexamethasone release rate (from $D_2$) | µg/h | $R*D_1*F_{loss}*k_1$ |
| $k_1$ | Release rate constant 1 | 1/h | 0.1018 (from *in vitro* release study) 0.03821 (from *in vivo* plasma data) |
| $k_2$ | Release rate constant 2 | 1/h | 0.0006235 |
| $F_{loss}$ | Non-absorbed drug fraction | – | 0.456 |
| $A_s$ | Amount of non-dissolved silica | µg | Initially 25 000 |
| $A_{s,\ diss}$ | Amount of dissolved silica (as silicic acid) in the subconjunctival space | µg | Simulated model variable |
| $J_{s,\ diss}$ | Rate of silica dissolution in the subconjunctival space | µg/h | $k_{d,\ in\ vitro}*A_s*R$ |
| $C_{si}$ | Concentration of dissolved silica in the subconjunctival space | µg/ml | $A_{s,\ diss}/V_{sc}$ |
| $V_{sc}$ | Volume of subconjunctival space | ml | 0.5 |
| $J_{s,el}$ | Elimination rate of dissolved silicic acid from subconjunctival space | µg/h | $A_s\ k_{10}$ |
| $k_{d,in\ vitro}$ | Rate constant for silica dissolution | 1/h | Initially 0.0519 |
| R | Restrictor of silica dissolution based on partial loss of sink conditions | – | $(S– C_{si})/S$ |
| $k_{10}$ | Rate constant for silicic acid elimination from subconjunctival space | 1/h | 7 |
| S | Water-solubility of silica | µg/ml | 130 |

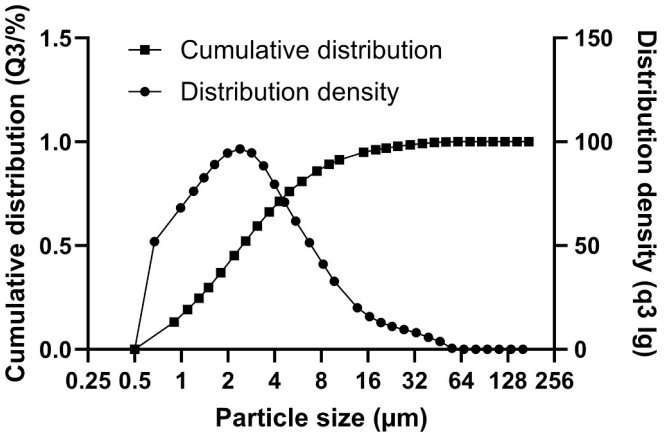


**Fig. 2.** Particle size distribution (mass distribution) of dexamethasone-silica microparticles measured with static light scatter from microparticle suspension as triplicate measurements in ethanol.

The rheological properties were studied using small angle oscillatory measurements in the linear viscoelastic region (Fig. 3). These measurements showed a three-dimensional gel structure within the hydrogel. The loss factor (tan $\delta = \acute{G}/\acute{G}$) was less than 1, indicating the viscoelastic nature of the hydrogel, where solid phase represents the continuous phase that dominate its elastic properties (Fan et al., 2022; Yan and Pochan, 2010). That is seen as similar oscillation measurement data before and after the shear stress (Fig. 3), demonstrating that non-flowing gel. The loss factor profiles of Fig. 3 (curves A, B and C), show that the material would not change significantly upon shear rate and shear stress induced in the injection needle. The result suggests that the formulation structure should be maintained after silica-hydrogel depot

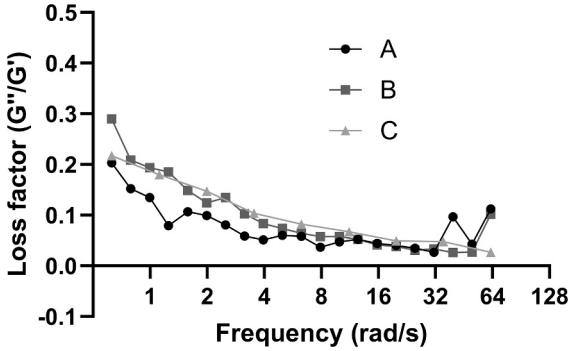


**Fig. 3.** Tangent Delta of Oscillation measurements of silica-dexamethasone hydrogel prior (A) and after (B) rotational shear thinning of the material and after manual shear stress induced with 23 G regular wall needle injection (C). N is 3 in all measurements. One outliner was removed from the A at 0.791 rad/s. Mean values are shown.

injection into subconjunctival space.

The shear thinning of the hydrogel was confirmed with viscosity measurements (Fig. 4). As the shear rate increased, the viscosity of the formulation decreased, which is typical for shear thinning materials. Upon higher shear rate, the gel reorientates and aligns in the direction of the shear. This shear thinning behavior allows easy injection of the hydrogel depot through thin needles, followed by its setting as a gel at the site of administration. The shear thinning behavior was further confirmed by manual injectability test that demonstrated injectability of hydrogel depot through a 23 G needle with minimal force. (Barnes, 1997).

The pH of the formulation was 5.8, which is within a suitable range to promote gelation and local tolerance in the eye (Wu et al., 2011).

### 3.3. *In vitro drug release and dissolution of silica*

*In vitro* dissolution testing of silica-hydrogel depot was carried out *in sink* conditions to avoid saturation of the dissolution sample by silicic acid which is the primary dissolution product of silica (Block et al., 2025; Kortesuo et al., 2000; Sun et al., 2020; Viitala et al., 2005b). This saturation is achieved already at silicic acid concentration of 0.1 mg/ml and it would stop the dissolution of silica matrix as well as drug release (Iler, 1979). Fig. 5 illustrates the cumulative *in vitro* release of dexamethasone and silica from the hydrogel formulation. About 87 ± 7 % of dexamethasone and 85 ± 10 % of silica were released in 24 h. Only a minor burst of non-encapsulated dexamethasone (1.7 %) was seen, confirming high drug encapsulation in the matrix. In the beginning, dissolution rate of silica was slower than the release rate of dexamethasone. This difference may be caused by location of dexamethasone closer to the surface of the silica microparticles.

*In vivo*, local concentration of silicic acids around the depot differs markedly from those *in sink* conditions which causes longer dissolution times *in vivo* compared to *in vitro*. Dissolution *in vivo* is a complex process, involving both the gradual conversion of silica into soluble silicic acid and the simultaneous clearance of this dissolved fraction from the injection site (Iler, 1979; Spitzmüller et al., 2023).

Therefore, while *sink* conditions facilitate the detection of formulation-specific differences in release profiles, and accelerates formulation development, this method may not fully capture the limitations imposed by low solubility under physiological conditions.

### 3.4. *Pharmacokinetics in rabbits after subconjunctival injection*

**Tear fluid analyses.** Dexamethasone was detected in the rabbit tear fluid 24 h after injection, whereas silica was quantitated for 26 days (Table 2).

This difference may arise from sample handling process and differences in clearance of dexamethasone and silica from the tear fluid. Prior to analysis, dexamethasone samples were processed with organic solvents that do not dissolve silica fragments with the drug. In case that a tear fluid sample contained subvisible fragments of the silica-hydrogel depot, some entrapped drug in silica may have been discarded prior to LC-MS analysis, and only the released fraction of dexamethasone is quantitated. In contrast, silica samples were processed with water-based solvents allowing quantitation of total silica, including both dissolved silicic acid and possible silica particles. In addition, dexamethasone is absorbed rapidly to cornea and conjunctiva and its clearance from tear fluid is high (Balla et al., 2022) contributing to its lower levels in tear fluid, whereas silica particles and dissolved silica have much lower clearance from the tear fluid to the eye and systemic circulation. Furthermore, dexamethasone quantity in the silica-hydrogel depot was ~ 20 times less than silica content.

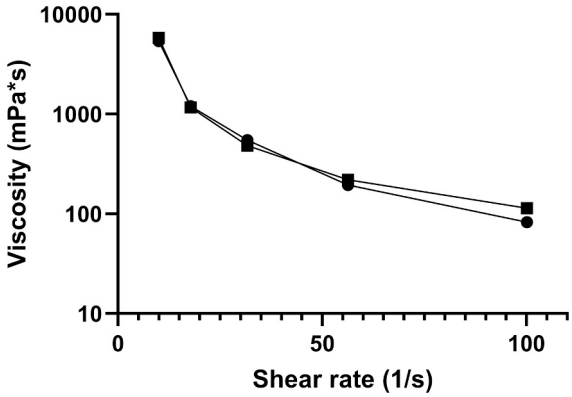


**Fig. 4.** Viscosity data of dexamethasone-silica hydrogel. N is 2.

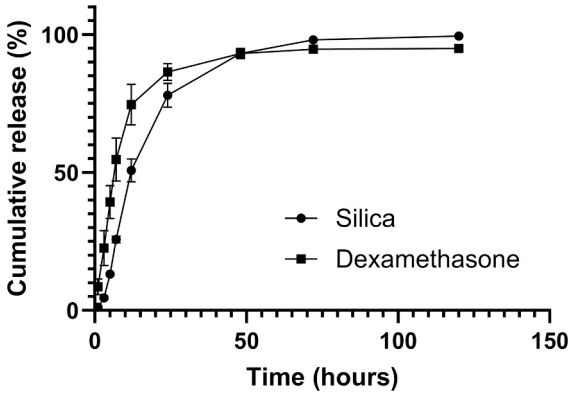


**Fig. 5.** *In vitro* release profiles of silica and dexamethasone in sink conditions from dexamethasone-silica hydrogel. The values represent means ± SD. N = 3.

**Table 2**
Dexamethasone and silica concentrations in tear fluid. Tear fluid samples from the right eyes were used for dexamethasone analysis and the samples from the left eyes were used for silica analysis (N = 3). NA = Not Analysed. < LOQ = limit of quantitation (<0.1 μg/ml).

| Time (hours) | Dexamethasone concentration | | Silica concentration | |
|---|---|---|---|---|
| | Average (μg/mL) | SD (μg/mL) | Average (μg/mL) | SD (μg/mL) |
| 0 | 0 | 0 | 0.95 | 1.65 |
| 1 | NA | NA | 9.18 | 8.41 |
| 3 | 0.53 | 0.80 | 20.45 | 13.46 |
| 3.5 | 0.73 | 0.74 | 23.28 | 5.60 |
| 24 | 0.12 | 0.11 | 30.15 | 18.80 |
| 96 | <LoQ | <LoQ | 23.69 | 17.10 |
| 168 | <LoQ | <LoQ | 24.39 | 19.86 |
| 264 | <LoQ | <LoQ | 12.27 | 4.56 |
| 336 | <LoD | <LoD | 29.75 | 21.67 |
| 480 | <LoD | <LoD | 18.43 | 1.23 |
| 624 | <LoD | <LoD | 0.95 | 1.65 |

**Analyses of aqueous and vitreous humour.** Aqueous and vitreous humour samples were collected 26 days after injection. Dexamethasone concentration in the vitreous humour was 0.73 ± 0.83 ng/mL (mean ± SD, range 0.32—2.18 ng/mL, N = 6). Since the threshold of active dexamethasone concentration in the vitreous humour is > 1 nM (> 0.393 ng/ml), active dexamethasone levels are maintained with silica-hydrogel depot for 26 days post-administration (Chang-Lin et al., 2011; Nauck et al., 1998; Sadeghi et al., 2022). In the aqueous humour dexamethasone concentrations were under the limit of quantitation (< 0.2 ng/mL) in all samples 26 days after injection. However, our calculations using dexamethasone bioavailability ($BA_{AH}$) in aqueous humour (0.74 %) and clearance ($CL_{AH}$) (13.6 μl/min) (Naageshwaran et al. 2022; Valtari et al. 2024) show that the dexamethasone levels during five days after injection are in the range 15–576 ng/ml. We calculated these values using release rate constant ($k_1$) from model B (0.03821 h-1) and

dexamethasone amount at time zero (1154 μg) and four days (29.46 μg) using equation CAH = (A * $k_1$ * BA) /CL, where A is the remaining amount in the depot. This is comparable to the levels after instillation of commercially available dexamethasone eyedrops (TobraDex®, TobraDexST®, and Maxidex®) which were reported to reach Cmax of 94.4, 90.4 and 72.3 ng/ml, respectively, and maintained the levels above 10 ng/ml during 6 h after eyedrop application.

**Plasma analyses.** Peak levels of dexamethasone in plasma were reached at 24 h post-injection (Fig. 6). $C_{max}$ was 8.6 ± 2.4 ng/mL (individual values 7.5, 11.4 and 7.0 ng/mL). Area under concentration vs time curves ($AUC_{0\text{-}26d}$) were 537.8, 752.3 and 550.4 ng*h/mL (mean ± SD was 613.5 ± 120.4, N = 3). Based on dexamethasone concentrations in plasma, drug release was faster during the first day and slower later on for 26 days.

**Depot remnant analyses.** Residual dexamethasone and silica in the hydrogel depot remnants were quantified at 26 days post-injection. The remaining dexamethasone content was 26 ± 6 % (mean ± SD, range 19–31 %, n = 6) of the original payload. Remaining silica content was 44 ± 8 % (mean ± SD, range 32–52 %, n = 6).

Overall, the pharmacokinetic data from plasma and tear fluid samples show biphasic release of dexamethasone from the silica-hydrogel depot: a faster release for 24 h, followed by a slower release for several weeks. The second phase is supported by the low sustained levels of dexamethasone in plasma (days 3–26) and its presence in the vitreous humour (day 26). Also, the remaining drug in the depot remnant (at day 26) suggest that not all dexamethasone was released in 26 days, and the dexamethasone release would go on at low level beyond 26 days. Compared to commercially available intravitreal dexamethasone implants (Ozurdex®), the concentration profile of our silica-hydrogel depot remains similar in nature; high initial concentration followed by lower concentration. However, the overall vitreal dexamethasone concentrations after Ozurdex are much higher (> 100 ng/ml during one month) than after subconjunctival depot (Bhagat et al., 2014; Won et al., 2024) it is not surprising that the vitreal dexamethasone levels are lower than after intravitreal injection, because large part of the subconjunctivally delivered drug is lost to systemic circulation (Ranta et al., 2010; Valtari et al., 2024). Dexamethasone levels at 26 days post-injection were above required threshold level for dexamethasone effects (≈ 1 nM). If these levels are effective *in vivo* subconjunctival depot might provide safer alternative to intravitreal injections. High ocular corticosteroid concentrations are associated with ocular adverse effects, especially cataract progression.

### 3.5. Simulations of drug release and pharmacokinetics

Simulation model for dexamethasone and silica release and pharmacokinetics model is shown schematically in Fig. 1 and the parameters are listed in Table 2. The model consists of systemic pharmacokinetics of dexamethasone (A), drug release from the silica-hydrogel depot (B), and dissolution of silica (C) (Fig. 1). These parts are interlinked with each other to describe overall *in vivo* performance of the silica-hydrogel depot.

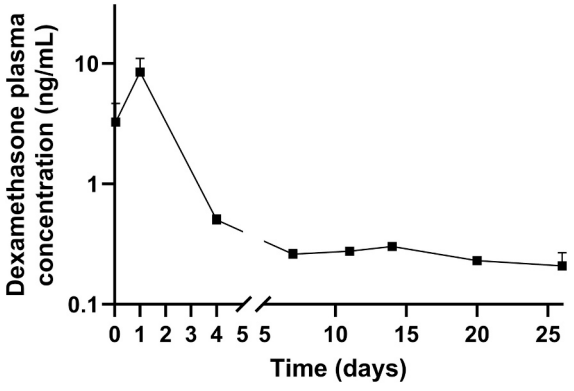


**Fig. 6.** Dexamethasone concentration in the rabbit plasma after subconjunctival injection of hydrogel. Mean ± SD values of 3 rabbits are shown.

**Section A: Systemic pharmacokinetic model.** The systemic pharmacokinetic model is based on the study of Valtari et al. (2024) for intravenous and subconjunctival administration of dexamethasone solutions to rabbits. Dexamethasone was rapidly absorbed from subconjunctival space to the rabbit circulation, where it obeyed two-compartmental kinetics (for parameters, see Table 2). Valtari et al (2024) validated the model against experimental dexamethasone concentrations in rabbits after intravenous and sub-conjunctival injections. Herein, the two-compartment model was built into STELLA simulation format and it was shown to perform as described by Valtari et al (2024).

**Section B: Dexamethasone release.** To describe sustained release from the hydrogel formulation, drug release was linked to the pharmacokinetic model (Fig. 1A and 1B). *In vivo* pharmacokinetics of dexamethasone in plasma indicated fast release for ≈4 days followed by slow release until 26 days post-injection (Fig. 6). Therefore, two compartments were introduced to the silica-hydrogel depot in the model (Table 2, Fig. 1). The whole dexamethasone payload in the injection (2041 μg) was divided to different parts: absorbed drug, residual drug (at 26 day), and released but non-absorbed dexamethasone loss.

Absorbed dexamethasone amount ($A_{abs}$) can be estimated based in AUC in plasma and clearance of dexamethasone: $A_{abs}$ = CL x $AUC_{0\text{-}26d}$ = 580 μg, where CL is 0.943 L/h and $AUC_{0\text{-}26d}$ is 614 ± 120 h·ng/mL (mean ± SD). Then, fast and slow releasing depot fractions can be estimated based on $AUC_{0\text{-}4d}$ (469.4 h·ng/mL) and $AUC_{4\text{-}26d}$ (144.9 h·ng/mL) as 443 μg (absorbed from $D_1$) and 137 μg (absorbed from $D_2$). Residual non-released content of dexamethasone was 530 μg at day 26 in the silica-hydrogel. Thus, formulation released 1511 μg (2041 μg– 530 μg) dexamethasone. The lost dexamethasone quantity was calculated by subtracting the known amounts (absorbed drug from $D_1$ and $D_2$ plus residual at day 26, in total 1110 μg) from total dexamethasone (2041 μg) yielding 931 μg. Thus, from both depot compartments 45.6 % is lost and 54.4 % absorbed to plasma. The loss may be due to formulation loss to tear fluid and outside of the eye. Thus, we can divide the unaccounted drug to fast ($D_1$) and slow ($D_2$) releasing fractions in the proportions as they are absorbed. Thus, $D_1$ (1154 μg) consists of rapidly absorbed quantity (443 μg) and proportional fraction of lost drug (711 μg), whereas $D_2$ (887 μg) is composed of slowly absorbed drug (137 μg), its fraction of lost drug (220 μg), and unreleased quantity (530 μg).

The rate constants for dexamethasone release *in vivo* were estimated from dexamethasone concentrations in plasma using semi-logarithmic first-order kinetics where declining slope of logC vs time data represents slowing first-order release rate. This approach assumes that the release kinetics from silica-hydrogel depot controls dexamethasone profiles in plasma. This is well established approach in first-order pharmacokinetics and allows extraction of the release rate constant from the declining slopes of plasma kinetics (Dash et al., 2010; Silva et al., 2015). The fast-releasing phase is described by $k_1$ value of 0.03821 $h^{-1}$, whereas the rate constant for slow-release phase ($k_2$) was 0.0006235 $h^{-1}$. The linearity of the log-transformed data confirmed that both release phases obeyed first-order kinetics, consistent with a process where the release rate is proportional to the remaining drug in the depot.

These results indicate that Depot 1 was depleted within the study period, while Depot 2 exhibited markedly slower release and retained a substantial part of the drug (530 μg) at the end of the study. Simulations based on these parameters (Sections A and B) successfully reproduced the observed plasma concentration–time profile, but the profile deviated slightly from the experimental datapoints (Fig. 7). This approach requires pharmacokinetic data for deriving the rate constants. Therefore, an case specific *in vivo* experiment is needed to obtain drug specific parameters for further predictions for formulation optimisation. Thus, this approach can reduce the need for extensive iterative animal experiments.

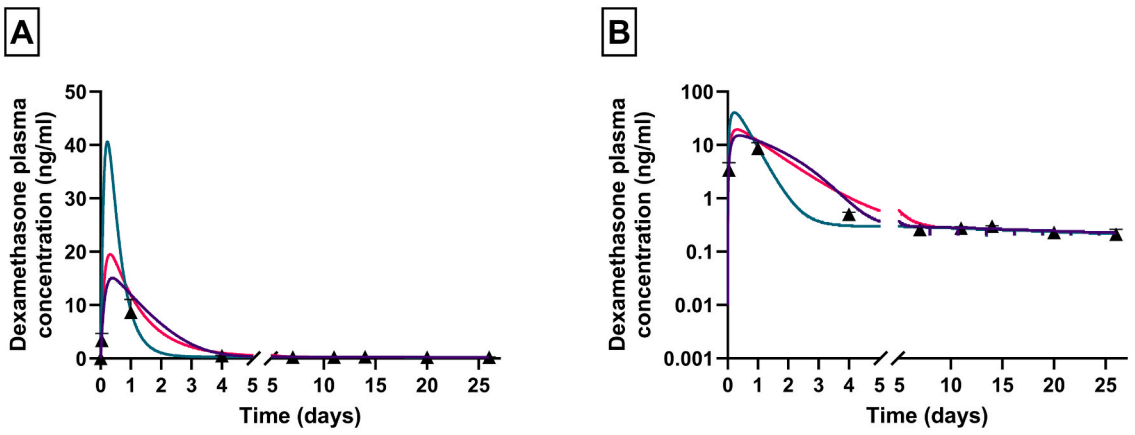


**Fig. 7.** Plasma concentrations of dexamethasone after subconjunctival delivery in silica hydrogel depot on linear (A) and semi-logarithmic (B) scales. The black triangles show experimental data. Red line indicates simulations based on release rate constants that have been derived from plasma curves. Green line shows simulation in which release rate is the same as *in vitro* experiment. Purple line shows simulation with restrictor that takes into account partial loss of sink-conditions in the sub-conjunctival space.

In order to build a predictive modelling approach and to reach *in vitro – in vivo* extrapolation, we used *in vitro* release rate constant ($k_1$ = 0.1018 $h^{-1}$) in the model as the initial value for the rate constant. In this case, the simulations resulted in peak dexamethasone concentrations that were about four times higher than the experimental peak levels in plasma (Fig. 7). Therefore, dexamethasone release in sub-conjunctival space does not take place as in sink conditions. It seems that the drug release and silica dissolution is taking place in non-sink conditions. It is known that for silica-hydrogel depots that dissolution of silica and build-up of silicic acid concentration in the dissolution medium slow down drug release rate and dissolution of silica (Iler, 1979; Viitala et al., 2005b).

**Section C: Non-sink conditions limiting silica dissolution and dexamethasone release.** Dissolution of silica and concentration build-up of silicic acid were added to the model using a third component (Fig. 1C). The added part accounts for the influence of silica dissolution on dexamethasone release from the silica-hydrogel depot in the sub-conjunctival space.

Dexamethasone was physically entrapped within silica-hydrogel, whose dissolution controls the rate of drug release. Solubility of silica in water is about 130–150 μg/mL at 37 °C (Iler, 1979; Viitala et al., 2005a). Once the local concentration of soluble silica approaches this solubility limit, further silica dissolution slows down, and it stops completely at saturation solubility level. Therefore, 130 μg/ml was used as the upper limit for solubility at which the release would stop.

The restrictor parameter was defined as R = ($S\text{-}C_{si}$)/S, where S = water solubility of silica and $C_{si}$ = concentration of dissolved silica when at *sink*. Restrictor term was used in the model to restrict dissolution of silica and release of dexamethasone. At *sink* condition $0 < R < 1$, while R = 0 when dissolved silica levels reach solubility level and release stops. In the simulations, the initial rates of silica dissolution (0.0519 $h^{-1}$) and dexamethasone release (0.1018 $h^{-1}$) were used based on *in vitro* experiments at *sink* conditions, but at later times the restrictor term will decrease the simulated *in vivo* release rate. Fig. 8 shows how restrictor modifies the simulated dexamethasone levels with full model presented in Fig. 1 (ABC), so that the initial peak levels are reduced to match experimentally measured values. Simulated dissolved silica levels in the subconjunctival space are in the range of 85 ± 5 μg/ml (mean ± SD) during 0.04——66 hrs post-injection, thereby showing that the sink conditions are partially lost during the initial fast release period. Later, sink conditions prevailed but the release rate was slow for other reasons.

Overall, our simulation work integrates together *in vitro* experiments with *in vivo* pharmacokinetics, thereby enabling predictions of dexamethasone release rates and pharmacokinetics in non-sink conditions in the sub-conjunctival space.

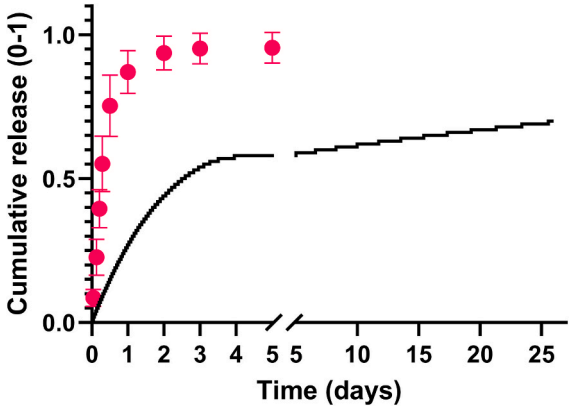


**Fig. 8.** Release of dexamethasone *in vitro* (red dots, N = 3, mean and SD) and simulated *in vivo* (black line) in partial sink conditions.

As demonstrated here, the silica-hydrogel formulation follows two distinct release phases clearly observable *in vivo*. This behaviour might be based on complex phenomenon derived both from material specific properties and of body's reaction towards injection. Currently, the dissolution method used *in vitro* cannot fully predict these properties very well and distinct methods would be needed to match the *in vivo* better. However, as at the beginning of the dissolution *in vivo* the conditions are allowing similar dissolution which is why the initial release parameters were able to be derived from *in vitro* testing as it is here. Thus, it would be beneficial to test these types of formulations in conditions allowing the concentration gradient of silica to have an effect in the release. Our results might help to indicate the volume and flow rate of such system that has meaningful ratios to have predictive value *in vivo*.

## 4. Conclusion

We show manufacturing, characterization and preclinical *in vivo* testing of silica-hydrogel formulation utilizing dexamethasone as a drug cargo molecule. The data shows dexamethasone release for at least 26 days as indicated by the drug levels found in the rabbit plasma and vitreous. A simulation model was developed for sub-conjunctival drug release systems. The model shows the interplay of silica dissolution and drug release in the subconjunctival space, and it is a useful tool for *in vitro – in vivo* extrapolation of silica-based hydrogel depots. Overall, silica matrix is an interesting alternative for drug carrier material for

prolonged drug release in the sub-conjunctival space.

## Funding sources

The work was supported by DelSiTech Ltd.

## Declaration of generative AI and AI-assisted technologies in the manuscript preparation process

During the preparation of this work the author(s) used Microsoft 365 Copilot© in order to enhance clarity of text. After using this tool, the author(s) reviewed and edited the content as needed and take(s) full responsibility for the content of the published article.

## CRediT authorship contribution statement

**Ville-Matias Pollari:** Writing – review & editing, Writing – original draft, Visualization, Validation, Software, Methodology, Investigation, Formal analysis, Data curation, Conceptualization. **Annika Valtari:** Writing – review & editing, Methodology, Formal analysis, Data curation. **Lauri Marttila:** Writing – review & editing, Validation, Methodology, Data curation. **Kati-Sisko Vellonen:** Writing – review & editing, Validation, Software, Methodology, Formal analysis, Data curation. **Marceline Akieh-Pirkanniemi:** Writing – review & editing, Supervision, Resources. **Mika Jokinen:** Writing – review & editing, Visualization, Supervision, Resources, Project administration, Funding acquisition, Conceptualization. **Lasse Leino:** Writing – review & editing, Visualization, Supervision, Resources, Project administration, Funding acquisition, Conceptualization. **Astrid Subrizi:** Writing – review & editing, Visualization, Supervision, Resources, Project administration, Funding acquisition, Conceptualization. **Arto Urtti:** Writing – review & editing, Visualization, Validation, Supervision, Software, Resources, Project administration, Methodology, Investigation, Funding acquisition, Conceptualization.

## Declaration of competing interest

The authors declare the following financial interests/personal relationships which may be considered as potential competing interests: Ville-Matias Pollari reports financial support was provided by DelSiTech Ltd. Lasse Leino reports a relationship with DelSiTech Ltd that includes: employment. Mika Jokinen reports a relationship with DelSiTech Ltd that includes: employment. Ville-Matias Pollari reports a relationship with DelSiTech Ltd that includes: employment. Lauri Marttila reports a relationship with DelSiTech Ltd that includes: employment. Marceline Akieh-Pirkanniemi reports a relationship with DelSiTech Ltd that includes: employment. Mika Jokinen has patent #US 9,949,922 B2 issued to U.S. Patent. If there are other authors, they declare that they have no known competing financial interests or personal relationships that could have appeared to influence the work reported in this paper.

## Acknowledgements

The authors would want to thank and acknowledge Lea Pirskanen and Matti Kaimainen for their technical assistance.

## Appendix A. Supplementary data

Supplementary data to this article can be found online at https://doi.org/10.1016/j.ijpharm.2026.126735.

## Data availability

Data will be made available on request.

## References

Al-Kinani, A.A., Zidan, G., Elsaid, N., Seyfoddin, A., Alani, A.W.G., Alany, R.G., 2018. Ophthalmic gels: past, present and future. Adv. Drug Deliv. Rev. 126, 113–126. https://doi.org/10.1016/j.addr.2017.12.017.

Annala, A., Sadeghi, A., Toropainen, E., Valtari, A., Puranen, J., Paterno, J.J., Pirskanen, L., Vellonen, K.-S., Hennink, W.E., Ruponen, M., Vermonden, T., Urtti, A., 2025. Intravitreal sustained release of dexamethasone from a self-healing injectable hydrogel: an in vivo safety and release study. Mol. Pharm. 22, 6920–6931. https://doi.org/10.1021/acs.molpharmaceut.5c00872.

Balla, A., Ruponen, M., Valtari, A., Toropainen, E., Tuomainen, M., Alvarez-Lorenzo, C., del Amo, E.M., Urtti, A., Vellonen, K.-S., 2022. Understanding dexamethasone kinetics in the rabbit tear fluid: drug release and clearance from solution, suspension and hydrogel formulations. Eur. J. Pharm. Biopharm. 172, 53–60. https://doi.org/10.1016/j.ejpb.2022.01.005.

Barnes, H.A., 1997. Thixotropy—a review. J. Nonnewton. Fluid Mech. 70, 1–33. https://doi.org/10.1016/S0377-0257(97)00004-9.

Benkő, F., Kristó, K., Sovány, T., 2025. Mesoporous silica nanoparticles as drug delivery systems. Pharmaceuticals 18, 1392. https://doi.org/10.3390/ph18091392.

Bhagat, R., Zhang, J., Farooq, S., Li, X.-Y., 2014. Comparison of the release profile and pharmacokinetics of intact and fragmented dexamethasone intravitreal implants in rabbit eyes. J. Ocul. Pharmacol. Ther. 30, 854–858. https://doi.org/10.1089/jop.2014.0082.

Block, M., Grube, A., Göpferich, A., Saal, C., Ilochonwu, B.C., Cárcamo-Martínez, Á., Giorgio, G., Bakker, R.A., Deanne, R., Schäfer, J., Walder, B.J., Simon, R., 2025. Surface-coated silica microparticles: in vitro and ex vivo evaluation of a preclinical extended release platform conceived for intravitreal injection. J. Control. Release 381, 113602. https://doi.org/10.1016/j.jconrel.2025.113602.

Chan, A., Leung, L.-S., Blumenkranz, M.S., 2011. Critical appraisal of the clinical utility of the dexamethasone intravitreal implant (Ozurdex®) for the treatment of macular edema related to branch retinal vein occlusion or central retinal vein occlusion. Clin. Opthalmolol. 5, 1043. https://doi.org/10.2147/OPTH.S13775.

Chang-Lin, J.-E., Attar, M., Acheampong, A.A., Robinson, M.R., Whitcup, S.M., Kuppermann, B.D., Welty, D., 2011. Pharmacokinetics and pharmacodynamics of a sustained-release dexamethasone intravitreal implant. Invest. Opthalmolol. vis. Sci. 52, 80. https://doi.org/10.1167/iovs.10-5285.

Coradin, T., Eglin, D., Livage, J., 2004. The silicomolybdic acid spectrophotometric method and its application to silicate/biopolymer interaction studies. J. Spectrosc. 18, 567–576. https://doi.org/10.1155/2004/356207.

Dash, S., Murthy, P.N., Nath, L., Chowdhury, P., 2010. Kinetic modeling on drug release from controlled drug delivery systems. Acta Pol. Pharm. 67, 217–223.

Fan, Z., Cheng, P., Zhang, P., Zhang, G., Han, J., 2022. Rheological insight of polysaccharide/protein based hydrogels in recent food and biomedical fields: a review. Int. J. Biol. Macromol. 222, 1642–1664. https://doi.org/10.1016/j.ijbiomac.2022.10.082.

Forsback, A.-P., Noppari, P., Viljanen, J., Mikkola, J., Jokinen, M., Leino, L., Bjerregaard, S., Borglin, C., Halliday, J., 2021. Sustained in-vivo release of triptorelin acetate from a biodegradable silica depot: comparison to pamorelin® LA. Nanomaterials 11, 1578. https://doi.org/10.3390/nano11061578.

Gaudana, R., Ananthula, H.K., Parenky, A., Mitra, A.K., 2010. Ocular drug delivery. AAPS J. 12, 348–360. https://doi.org/10.1208/s12248-010-9183-3.

Go, E.J., Kang, E.Y., Lee, S.K., Park, S., Kim, J.H., Park, W., Kim, I.H., Choi, B., Han, D.K., 2020. An osteoconductive PLGA scaffold with bioactive β-TCP and anti-inflammatory Mg(OH) $_2$ to improve *in vivo* bone regeneration. Biomater. Sci. 8, 937–948. https://doi.org/10.1039/C9BM01864F.

Goñi, F.J., Stalmans, I., Denis, P., Nordmann, J.-P., Taylor, S., Diestelhorst, M., Figueiredo, A.R., Garway-Heath, D.F., 2016. Elevated intraocular pressure after intravitreal steroid injection in diabetic macular edema: monitoring and management. Ophthalmol. Ther. 5, 47–61. https://doi.org/10.1007/s40123-016-0052-8.

Grzybowski, A., Brockmann, T., Kanclerz, P., Pleyer, U., 2019. Dexamethasone intraocular suspension: a long-acting therapeutic for treating inflammation associated with cataract surgery. J. Ocul. Pharmacol. Ther. 35, 525–534. https://doi.org/10.1089/jop.2019.0072.

Iler, R., 1979. The chemistry of silica. John Wiley & Sons, New York.

Järvinen, K., Järvinen, T., Urtti, A., 1995. Ocular absorption following topical delivery. Adv. Drug Deliv. Rev. 16, 3–19. https://doi.org/10.1016/0169-409X(95)00010-5.

Jokinen, M., Jalonen, H., Forsback, A.-P., 2018. Silica Hydrogel Composite. US 9,949,922 B2.

Kiddee, W., Trope, G.E., Sheng, L., Beltran-Agullo, L., Smith, M., Strungaru, M.H., Baath, J., Buys, Y.M., 2013. Intraocular pressure monitoring post intravitreal steroids: a systematic review. Surv. Ophthalmol. 58, 291–310. https://doi.org/10.1016/j.survophthal.2012.08.003.

Kortesuo, P., Ahola, M., Karlsson, S., Kangasniemi, I., Yli-Urpo, A., Kiesvaara, J., 2000. Silica xerogel as an implantable carrier for controlled drug delivery—evaluation of drug distribution and tissue effects after implantation. Biomaterials 21, 193–198. https://doi.org/10.1016/S0142-9612(99)00148-9.

Lu, Y., Cheng, D., Niu, B., Wang, X., Wu, X., Wang, A., 2023. Properties of poly (lactic-co-glycolic acid) and progress of poly (lactic-co-glycolic acid)-based biodegradable materials in biomedical research. Pharmaceuticals 16, 454. https://doi.org/10.3390/ph16030454.

McGowan, A., Gennemark, P., Akieh-Pirkanniemi, M., Wirman, L., Davies, N., Elebring, M., Tivesten, A., Strimfors, M., Hölttä, M., Söderberg, M., Berntsson, V., Balas, D., Koskinen, M., Leino, L., Abrahmsén-Alami, S., 2024. Injectable biodegradable silica depot for controlled subcutaneous delivery of antisense

oligonucleotides with beyond monthly administration. Mol. Pharm. 21, 143–151. https://doi.org/10.1021/acs.molpharmaceut.3c00663.
Naageshwaran, V., Ranta, V.-P., Toropainen, E., Tuomainen, M., Gum, G., Xie, E., Bhoopathy, S., Urtti, A., del Amo, E.M., 2022. Topical pharmacokinetics of dexamethasone suspensions in the rabbit eye: bioavailability comparison. Int. J. Pharm. 615, 121515. https://doi.org/10.1016/j.ijpharm.2022.121515.
Nauck, M., Karakiulakis, G., Perruchoud, A.P., Papakonstantinou, E., Roth, M., 1998. Corticosteroids inhibit the expression of the vascular endothelial growth factor gene in human vascular smooth muscle cells. Eur. J. Pharmacol. 341, 309–315. https://doi.org/10.1016/S0014-2999(97)01464-7.
Noppari, P., Jokinen, M., Dargelas, F., Mikkola, J., Leino, L., 2021. CHAPTER 9. Parenteral Delivery of Therapeutic Proteins, Peptides and Small Molecules Using Biodegradable Silica. pp. 188–215. https://doi.org/10.1039/9781839164958-00188.
Rafiei, F., Tabesh, H., Farzad, F., 2020. Sustained subconjunctival drug delivery systems: current trends and future perspectives. Int. Ophthalmol. 40, 2385–2401. https://doi.org/10.1007/s10792-020-01391-8.
Ranta, V.-P., Mannermaa, E., Lummepuro, K., Subrizi, A., Laukkanen, A., Antopolsky, M., Murtomäki, L., Hornof, M., Urtti, A., 2010. Barrier analysis of periocular drug delivery to the posterior segment. J. Control. Release 148, 42–48. https://doi.org/10.1016/j.jconrel.2010.08.028.
Ranta, V.-P., Urtti, A., 2006. Transscleral drug delivery to the posterior eye: prospects of pharmacokinetic modeling. Adv. Drug Deliv. Rev. 58, 1164–1181. https://doi.org/10.1016/j.addr.2006.07.025.
Rungseevijitprapa, W., Bodmeier, R., 2009. Injectability of biodegradable in situ forming microparticle systems (ISM). Eur. J. Pharm. Sci. 36, 524–531. https://doi.org/10.1016/j.ejps.2008.12.003.
Sadeghi, A., Ruponen, M., Puranen, J., Cao, S., Ridolfo, R., Tavakoli, S., Toropainen, E., Lajunen, T., Ranta, V.-P., van Hest, J., Urtti, A., 2022. Imaging, quantitation and kinetic modelling of intravitreal nanomaterials. Int. J. Pharm. 621, 121800. https://doi.org/10.1016/j.ijpharm.2022.121800.
Silva, B., São Braz, B., Delgado, E., Gonçalves, L., 2021. Colloidal nanosystems with mucoadhesive properties designed for ocular topical delivery. Int. J. Pharm. 606, 120873. https://doi.org/10.1016/j.ijpharm.2021.120873.
Silva, L., Pereira, J., Ramalho, A., Ferreira, D., 2015. Mathematical models of drug release, in: Strategies to Modify the Drug Release from Pharmaceutical Systems. Elsevier, pp. 63–86. https://doi.org/10.1016/B978-0-08-100092-2.00005-9.
Spitzmüller, L., Nitschke, F., Rudolph, B., Berson, J., Schimmel, T., Kohl, T., 2023. Dissolution control and stability improvement of silica nanoparticles in aqueous media. J. Nanopart. Res. 25, 40. https://doi.org/10.1007/s11051-023-05688-4.
Sun, Y., Huffman, K., Freeman, W.R., Sailor, M.J., Cheng, L., 2020. Intravitreal safety profiles of sol-gel mesoporous silica microparticles and the degradation product (Si(OH)$_4$. Drug Deliv. 27, 703–711. https://doi.org/10.1080/10717544.2020.1760401.
Thorne, J.E., Woreta, F.A., Dunn, J.P., Jabs, D.A., 2010. Risk of cataract development among children with juvenile idiopathic arthritis-related uveitis treated with topical corticosteroids. Ophthalmology 117, 1436–1441. https://doi.org/10.1016/j.ophtha.2009.12.003.
Thrimawithana, T.R., Young, S., Bunt, C.R., Green, C., Alany, R.G., 2011. Drug delivery to the posterior segment of the eye. Drug Discov. Today 16, 270–277. https://doi.org/10.1016/j.drudis.2010.12.004.
Tyagi, P., Koskinen, M., Mikkola, J., Leino, L., Schwarz, A., 2018. Silica microparticles for sustained zero-order release of an anti-CD40L antibody. Drug Deliv. Transl. Res. 8, 368–374. https://doi.org/10.1007/s13346-017-0408-1.
Tyagi, P., Koskinen, M., Mikkola, J., Sarkhel, S., Leino, L., Seth, A., Madalli, S., Will, S., Howard, V.G., Brant, H., Corkill, D., 2022. Injectable biodegradable silica depot: two months of sustained release of the blood glucose lowering peptide. Pramlintide. Pharmaceutics 14, 553. https://doi.org/10.3390/pharmaceutics14030553.
Valtari, A., Posio, S., Toropainen, E., Balla, A., Puranen, J., Sadeghi, A., Ruponen, M., Ranta, V.-P., Vellonen, K.-S., Urtti, A., del Amo, E.M., 2024. Comprehensive ocular and systemic pharmacokinetics of dexamethasone after subconjunctival and intravenous injections in rabbits. Eur. J. Pharm. Biopharm. 198, 114260. https://doi.org/10.1016/j.ejpb.2024.114260.
Viitala, R., Jokinen, M., Maunu, S.L., Jalonen, H., Rosenholm, J.B., 2005a. Chemical characterization of bioresorbable sol–gel derived SiO2 matrices prepared at protein-compatible pH. J. Non Cryst. Solids 351, 3225–3234. https://doi.org/10.1016/j.jnoncrysol.2005.08.023.
Viitala, R., Jokinen, M., Tuusa, S., Rosenholm, J.B., Jalonen, H., 2005b. Adjustably bioresorbable sol-gel derived SiO2 matrices for release of large biologically active molecules. J. Solgel Sci. Technol. 36, 147–156. https://doi.org/10.1007/s10971-005-5286-1.
Walvekar, P., Kumar, P., Choonara, Y.E., 2023. Long-acting vaccine delivery systems. Adv. Drug Deliv. Rev. 198, 114897. https://doi.org/10.1016/j.addr.2023.114897.
Wang, X., Bao, Q., Wang, R., Kwok, O., Maurus, K., Wang, Y., Qin, B., Burgess, D.J., 2023. In situ forming risperidone implants: effect of PLGA attributes on product performance. J. Control. Release 361, 777–791. https://doi.org/10.1016/j.jconrel.2023.08.029.
Wang, Y., Otte, A., Park, H., Park, K., 2025. In vitro-in vivo correlation (IVIVC) development for long-acting injectable drug products based on poly(lactide-co-glycolide). J. Control. Release 377, 186–196. https://doi.org/10.1016/j.jconrel.2024.11.021.
Won, J., Kang, J., Kang, W., 2024. Comparative ocular pharmacokinetics of dexamethasone implants in rabbits. J. Ocul. Pharmacol. Ther. 40, 608–614. https://doi.org/10.1089/jop.2024.0052.
Wu, H., Liu, Z., Peng, J., Li, L., Li, N., Li, J., Pan, H., 2011. Design and evaluation of baicalin-containing in situ pH-triggered gelling system for sustained ophthalmic drug delivery. Int. J. Pharm. 410, 31–40. https://doi.org/10.1016/j.ijpharm.2011.03.007.
Yan, C., Pochan, D.J., 2010. Rheological properties of peptide-based hydrogels for biomedical and other applications. Chem. Soc. Rev. 39, 3528. https://doi.org/10.1039/b919449p.
Zhang, L., Li, Y., Zhang, C., Wang, Y., 2009. Pharmacokinetics and tolerance study of intravitreal injection of dexamethasone-loaded nanoparticles in rabbits. Int. J. Nanomed. 4, 175–183. https://doi.org/10.2147/IJN.S6428.
Zhao, C., Zhu, Z., Cao, X., Pan, F., Li, F., Xue, M., Guo, Y., Zhao, Y., Zeng, J., Liu, Yu., Yang, Z., Liu, Y., Ren, F., Feng, L., 2023. Evaluation the injectability of injectable microparticle delivery systems on the basis of injection force and discharged rate. Eur. J. Pharm. Biopharm. 190, 58–72. https://doi.org/10.1016/j.ejpb.2023.06.017.